Desalination and Water Treatment
www.deswater.com
doi: 10.1080/19443994.2014.925834

55 (2015) 1598–1608
July

Taylor & Francis
Taylor & Francis Group

Adsorption property of methyl orange by chitosan coated on quartz sand in batch mode

Binglu Zhao, Xiaona Zhang, Chanchan Dou, Runping Han*

School of Chemistry and Molecular Engineering, Zhengzhou University, No 100 Kexue Road, Zhengzhou 450001, P.R. China, Tel. +86 371 67781757; Fax: +86 371 67781556; emails: rphan67@sohu.com (B. Zhao), 854975880@qq.com (X. Zhang), douchan317@126.com (C. Dou), rphan67@zzu.edu.cn (R. Han)

Received 18 October 2013; Accepted 14 May 2014

ABSTRACT

The adsorption behavior of methyl orange (MO) on chitosan-coated quartz sand (CCS) was studied as a function of initial solution pH, salt concentration, contact time, concentration of MO, and temperature in batch mode. The adsorption quantity of MO on CCS was 45.5 mg g^{-1} at 293 K under the conditions of pH 4.00, CCS dosage 1.00 g L^{-1}, and contact time 720 min. The high temperature and existence of common salts in solution were disadvantage of MO adsorption. The equilibrium data were fitted well to the Langmuir and Temkin isotherm models. Pseudo-first-order kinetic model, pseudo-second-order kinetic model, Elovich equation, and intra-particle diffusion models were used to fit the kinetic experimental data, and the fitted results showed that Elovich equation was the best to predict the kinetic process. The adsorption was spontaneous and exothermic, according to the thermodynamic parameters. It was concluded that ion exchange occurs mainly in the adsorption process. The dye-loaded adsorbent can be reused by regeneration with hot water.

Keywords: Chitosan-coated quartz sand; Methyl orange; Adsorption; Regeneration

1. Introduction

The removal of hazardous materials such as heavy metals, aromatic compounds, and dyes from industrial effluents is of great environmental concern. Dyes are common constituents of effluents discharged by various industries, such as dyestuffs, textile, paper and plastics, particularly the textile industry. There are over 100,000 commercially available dyes and more than 7×10^5 tones are produced annually [1,2]. The presence of small amounts of dyes in water is highly visible and undesirable [3]. Therefore, the effective treatment method of dyeing wastewater becomes a task of top priority to the government. Currently, several technologies have been developed, including adsorption, oxidation, super filter film, and coagulation, etc. [4,5]. However, all of these methods have various drawbacks, such as cost, inefficiency, and pollution. Adsorption technique is popular due to its simplicity, low cost, and easy operation. A successful adsorption process not only depends on pollutants' adsorption performance of the adsorbents, but also on the constant supply of the materials for the process. Certainly, activated carbon is the most effective adsorbent. However, high cost in production and regeneration makes it uneconomical. Many low-cost adsorbents were selected and the results confirmed that the adsorption technique was an effective and

*Corresponding author.

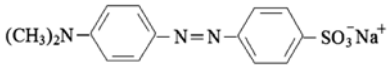

Fig. 1. Structure of MO.

attractive process for removal of non-biodegradable pollutants (including dyes) from wastewater [6–16].

In China, quartz sand is widely used as a filter in the production of tap water. Quartz sand can be used as a substrate or carrier for its stability, high hardness, and strength, but its adsorption capacity is very poor. The modified quartz sand was applied to adsorb bromate [17], arsenic [18], phosphorus, [19] and lead ion and copper ion [20] from solution.

Chitosan is a biopolymer with a linear polysaccharide based on glucosamine unit, which is easily prepared from chitin by deacetylating its acetoamide groups with a strong alkaline solution and is considered to be versatile and environmental friendly, which can be biosynthesized or biodegraded [21]. It is widely applied in the removal of metal ions [22–24] and organic dyes [25,26] because it contains large numbers of two functional groups (–OH and $–NH_2$). However, the drawbacks of granulation, low solubility in acid, and low density of chitosan limit its commercial application as an adsorbent. In previous studies, various types of solids have been coated by chitosan, such as bentonite [27,28], perlite [29], montmorillonite [30], activated clay [31], calcium alginate, silica [32], zeolite [33], and magnetic iron oxides [34]. Chitosan-coated quartz sand (CCS) was prepared and used to adsorb copper and lead ions [35,36]. CCS can not only foster strengths and circumvent weaknesses of chitosan, but also can enhance the adsorption capacity of sand. There seemed to be no report on the dye adsorption onto CCS.

Methyl orange (MO, C·I. 13,025, molecule weight 327.36 g mol^{-1}, CAS 547-58-0) is one of the well-known acidic/anionic dyes (structure shown in Fig. 1), and it has been widely used in textile, printing, paper, food, and pharmaceutical industries, and experimental laboratories. Therefore, the main objective of the present research is to investigate the property of MO adsorption onto CCS as a function of pH, salt concentration, contact time, MO concentration, and temperature. Adsorption isotherm models and kinetic equations were used to fit the experimental data, respectively.

2. Materials and methods

2.1. Preparation CCS

The method for the preparation of CCS has been described elsewhere [35,36]. Briefly, a proper amount of natural quartz sand (40–60 mesh) was first soaked in hydrochloric acid solution (1.0 mol L^{-1}) for 24 h, then washed with deionized water until the solution is neutral, dried at 373 K in an oven until its weight was constant. It was grounded to pass through 60–80 mesh sieves. 5 g chitosan was put into 300 ml of hydrochloric acid solution (pH 1.5) and quartz sand (100 g) was added to the solution and stirred for 5 h until the chitosan was dissolved completely. NaOH solution (pH 13.00) was dropped at stirred condition until it became into colloidal state. The mixtures were filtered, and the solids were washed repeatedly until the pH of the suspension became neutral. The solids were dried, grinded and sieved, and CCS was obtained. It was stored in an airtight glass container for experiment.

Elemental analysis showed that there were C 2.31%, N 0.46%, and H 0.40% in CCS while carbon, nitrogen, and hydrogen were not detected for sand. Through difference of weight before and heating at 550˚C in muffle oven, the percent of successful chitosan coating on sand is 4.5%. These results implied that chitosan can be successfully coated on the surface of sand.

2.2. Preparation of MO solution

The stock solution of MO (500 mg L^{-1}) was prepared in distilled water. All working solutions were prepared by diluting the stock solution with appropriate volume of distilled water. Solution pH was adjusted to 4.0 from the result of the effect of pH on MO adsorption. All reagents and chemicals used were of analytical grade.

2.3. Adsorption study

Batch adsorption tests were performed at different contact time at the initial constant concentration of MO and adsorbent dosage 0.02 g (except effect of adsorbent dose) in 20 ml solution at the temperature of 293 K. Agitation was made at a constant agitation speed of 120 rpm for 720 min. The samples were then taken out at certain time interval and filtrated. The remaining concentration of solution was analyzed by using a UV spectrophotometer (Shimadzu Brand UV-3000), by monitoring the absorbance changes at a wavelength of maximum absorbance (480 nm). The quantity of dye loaded onto unit weight of CCS (q_t or q_e, mg g^{-1}) and removal efficiency (R%) were obtained using the expression Eqs. (1) and (2), respectively:

$$q_e = \frac{(C_0 - C)v}{m} \quad (1)$$

$$R = \frac{C_0 - C}{C_0} \times 100\,\% \quad (2)$$

where C_0 is the initial concentration of MO (mg L^{-1}), C is the concentration of MO at any time t or equilibrium time (mg L^{-1}), V is the solution volume (L), and m is the mass of CCS (g), R is removal efficiency.

The effect of CCS dosage on the adsorption of MO onto CCS was conducted by contacting different dosage of CCS, 0.5–4.0 g L^{-1} with 20 ml MO solution (30 mg L^{-1}). MO solution was adjusted to pH of 2.00–10.00 to study the effect of initial solution pH on adsorption quantity.

2.4. Adsorption equilibrium study

Equilibrium experiments were carried out by mixing 0.02 g of CCS with 20 ml MO solution with different initial dye concentration. A series of conical flasks was then shaken in an oscillator with temperatures 293, 303, and 313 K, respectively. After 720 min, the samples were left out and filtrated to determine the concentration of MO in the solution.

Adsorption isotherms represent the interrelation between the values of C_e and q_e calculated at equilibrium, which is characterized by certain constants which values reveal the surface properties and display the affinity of an adsorbent for a particular adsorbate. Almost every model has linear and nonlinear forms. Indeed, different forms of the equation affected R^2 values more significantly during the linear analysis, the nonlinear analysis might be a method of avoiding such errors. Therefore, all model parameters were evaluated by nonlinear regression analysis in the present study.

The Langmuir model assumes that monolayer adsorption occurs on the solid surface with identical homogeneous sites [37]. It has been successfully applied to many pollutants' adsorption processes and has been the most widely used adsorption isotherm for the adsorption of a solute from a liquid solution. The expression of the Langmuir isotherm equation is represented as Eq. (3):

$$q_e = \frac{q_m K_L C_e}{1 + K_L C_e} \quad (3)$$

where q_m is the q_e for a complete monolayer (mg g^{-1}), and K_L is a constant related to the affinity of the binding sites and energy of adsorption (L mg^{-1}), q_e is sorption capacity at equilibrium (mg g^{-1}), C_e is equilibrium concentration of MO (mg L^{-1}).

The Freundlich isotherm [37] is an empirical equation employed to describe the heterogenous surface adsorption process and high adsorption properties, but can't describe the saturation behavior of the adsorbent. The isotherm equation is written as Eq. (4):

$$q_e = K_F C_e^{1/n} \quad (4)$$

where K_F and $1/n$ are the Freundlich constants related to the adsorption capacity and adsorption intensity of the adsorbent, respectively.

The derivation of the Temkin isotherm assumes that the fall in the heat of adsorption is linear rather than logarithmic, as implied in the Freundlich equation. It can also be applied to describe the heterogeneous surface adsorption as the Freundlich equation. The Temkin isotherm is expressed as Eq. (5) [37]:

$$q_e = A + B \ln C_e \quad (5)$$

where A and B are isotherm constants.

2.5. Kinetic studies

The kinetic data obtained from the batch adsorption at 303 K using 0.02 g of CCS in 20 ml of 30, 50, and 80 mg L^{-1} of MO were analyzed using four different kinetic models: pseudo-first-order equation, pseudo-second-order equation, Elovich equation and intra-particle diffusion equation.

The pseudo-first-order model [38] was the first rate equation for the adsorption of liquid/solid system based on solid capacity. It may be represented by Eq. (6):

$$q_t = q_e(1 - e^{-k_1 t}) \quad (6)$$

where q_e is the amount of dye adsorbed at equilibrium (mg g^{-1}), q_t is amount of dye adsorbed at time t (mg g^{-1}), k_1 is the equilibrium rate constant of pseudo-first adsorption (min^{-1}).

The pseudo-second-order model which was based on the assumption that the rate-limiting step may be chemical adsorption or chemisorption involving valency forces through sharing or exchange of electron between adsorbent and adsorbate [39]. The pseudo-second-order kinetic rate equation is expressed as Eq. (7):

$$q_t = \frac{k_2 q_e^2 t}{1 + k_2 q_e t} \quad (7)$$

where k_2 is the rate constant of the pseudo-second-order adsorption (mg g^{-1} min^{-1}).

The Elovich equation is a useful model for describing activated chemisorption. The Elovich equation is expressed as Eq. (8) [40]:

$$q_t = \frac{\ln(a\beta)}{\beta} + \frac{\ln t}{\beta} \quad (8)$$

where α (mg g^{-1} min^{-1}) is initial adsorption rate constant while β (g mg^{-1}) is desorption constant.

Intra-particle diffusion equation was applied to investigate whether the adsorption process was controlled by diffusion in the adsorbent particles and consecutive diffusion in the bulk of the solution. The intra-particle diffusion [41], an empirically found functional relationship, common to most adsorption processes, is that the uptake varies almost proportionally with $t^{1/2}$, rather than with the contact time t. It is expressed as Eq. (9):

$$q_t = K_t t^{1/2} + C \quad (9)$$

where K_t is diffusion rate constant (mg g^{-1} min$^{-0.5}$) and C is constant (mg g^{-1}).

2.6. Desorption and regeneration study

Desorption study can help in elucidating the mechanism of an adsorption process [42–44]. To make the adsorption process more economical, it is necessary to regenerate the spent CCS. The exhausted or dye-loaded CCS was obtained for the adsorption of 50 mg L^{-1} of MO at pH 4.00. The MO-loaded CCS was washed by distilled water to remove the residual dye and was dried at 353 K. The exhausted CCS was regenerated with 20 ml 0.1 mol L^{-1} NaOH, 0.1 mol L^{-1} $NaClO_3$ at 303 K and 0.1 mol L^{-1} NaCl, water at 333 K, respectively. The regenerated adsorbent was reused to adsorb MO from solution at the same experimental conditions. The regeneration yield was calculated as the ratio of values of q_e before and after regeneration.

3. Results and discussions

3.1. The adsorption comparison of CCS, pure quartz sand and chitosan to MO

The results of adsorption quantity per gram (q_e) at different shaking times were shown in Fig. 2.

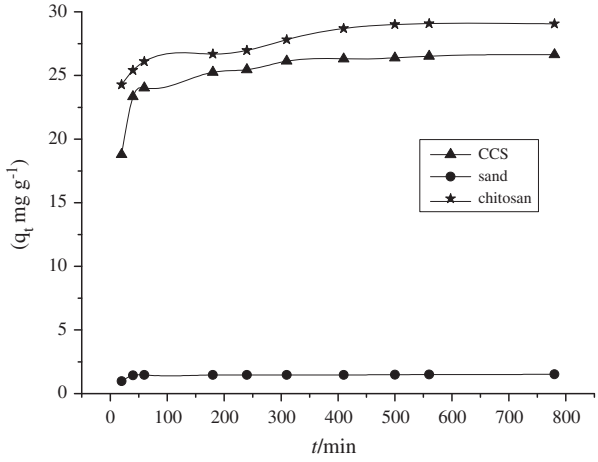

Fig. 2. Comparison of adsorption quantity among CCS, pure quartz sand, and chitosan to MO (dosage 1.0 g L^{-1}, C_0 = 30 mg L^{-1}, T = 303 K, and pH 4.00).

From Fig. 2, the adsorption capacity of CCS toward MO was better than that of natural quartz sand, slightly inferior to chitosan. Adsorption capacity of CCS was 20 times more than natural quartz sand in 180 min, and MO molecules can occupy adsorption sites on CCS surface quickly in the initial stage of adsorption. The active site or functional groups of –NH_2 and –OH was lower in one gram adsorbent of CSS which led to lower adsorption quantity(than chitosan). The use of chitosan alone is costly, because construction of filters requires more adsorbents. Immobilizing chitosan on a low-cost material can result in lower amounts of chitosan being used, but the overall adsorption capacity toward pollutants may not significantly be affected [35,36], especially about one gram of chitosan in composite. Moreover, the composites improve the mechanical strength and specific gravity compared to chitosan [34]. This can be advantage of application in real wastewater and CCS is better selected as an adsorbent.

According to Fig. 2, the contact time was constant at 720 min in order to guarantee the adsorption equilibrium.

3.2. Effect of CCS dosage

The effect of dosage on the removal of MO was illustrated in Fig. 3.

It was observed from Fig. 3 that the values of q_e decreased from 34.7 mg g^{-1} to 6.7 mg g^{-1},while the percentage removal efficiency (R) increased from 48.6 to 90.7% when the dosage increased from 0.5 to 4 g L^{-1}.

It can be explained that the active site available for MO adsorption increases with the increase of the

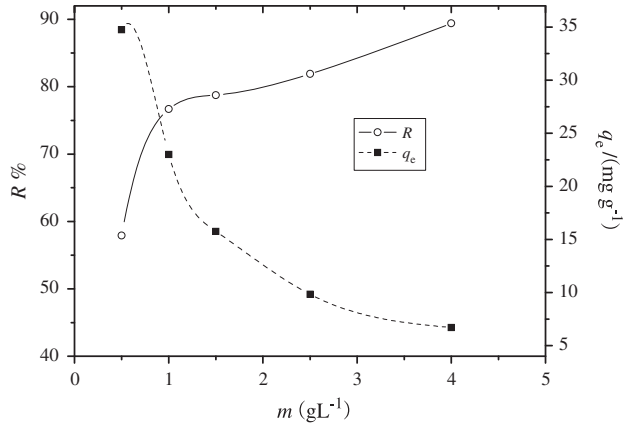

Fig. 3. Effect of CCS dosage on removal efficiency and adsorption quantity of MO ($C_0 = 30\ mg\ L^{-1}$, pH 4.00, contact time 720 min, and $T = 303\ K$).

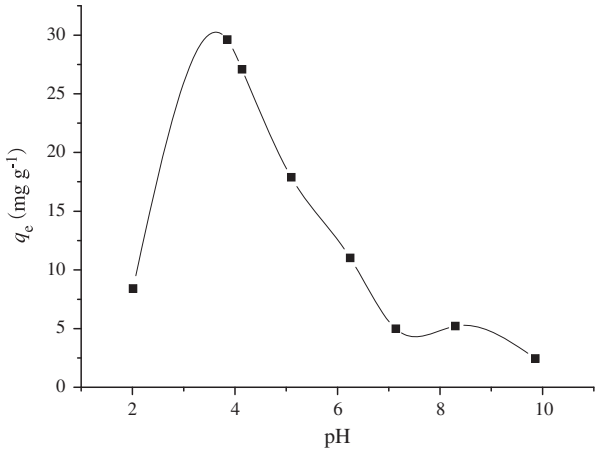

Fig. 4. Effect of solution pH on the adsorption quantity of MO ($C_0 = 30\ mg\ L^{-1}$, CCS dosage $1.0\ g\ L^{-1}$, contact time 720 min, and $T = 303\ K$).

adsorbent dose, and consequently, this produces a lower MO concentration in the solution. Thus, a higher value of R was observed. But, with increasing adsorbent dose, the amount of MO adsorbed per unit mass of CCS reduced, causing a decrease in q_e value. This may be attributed to overlapping or aggregation of adsorption sites resulting in a decrease in total adsorbent surface area available to the MO and an increase in diffusion path length [25]. Similar effect was previously reported [45,46]. The dosage of CCS $1.00\ g\ L^{-1}$ was selected in following experiments.

3.3. Effect of initial solution pH

It is known that the initial pH values of dye solutions affect the structure and properties of both the dye molecule and the adsorbent. Hence, it can affect the adsorption quantity. Fig. 4 showed the effect of solution pH on adsorption quantity of MO binding onto CCS.

It was observed that the optimum pH value was 4.0, lower or higher this value was adverse to the adsorption. The adsorption capacity increased with the pH value increasing at the range of 2.0–4.0, while, when the value of pH increased from 4.0 to 7.0, the adsorption quantity decreased. Moreover, adsorption quantity was approximately constant when the pH ranged from 7.0 to 10.0. Similar result was observed in the adsorption of MO onto chitosan [47]. Several reasons may be attributed to the adsorption behavior of CCS to MO. For one reason, chitosan was soluble in water at a lower pH, which lead to active adsorption sites decrease on adsorbent surface. At lower pH, more protons are available and amino groups at surface of chitosan molecules are protonated to form $-NH_3^+$ groups. This increased the electrostatic attractions between negatively charged dye anions (MO) and positively charged adsorption sites and increased dye adsorption [25]. The chitosan protonation was hindered and electrostatic attraction decreased along with the increase of pH, but CCS still adsorb MO molecules through the hydrogen bond and van der Waals force. In alkaline medium, there is a competition between the OH^- ions and the dye anions. It can be seen that the pH of aqueous solution plays an important role in the adsorption of anionic dyes onto chitosan. Further studies on adsorptive removal of MO by CCS were carried out at pH 4.0.

3.4. The effect of salinity on the adsorption

The common salt ions such as Na^+, Ca^{2+}, Cl^-, etc. with certain concentration were often existed in the actual industrial wastewater, so it was necessary to discuss the effects of salinity or ion strength on the adsorption process. Fig. 5 showed the effect of NaCl concentration on adsorption quantity.

From Fig. 5, the existence of NaCl in solution was not favor of MO adsroption. The adsorption quantity of CCS toward MO reduced rapidly and then tended to be stable with the increase of the concentration of NaCl from 0 to $0.20\ mol\ L^{-1}$, which could be attributed to the competitive effect between MO ions and anionic from the salt for the available sites at adsorbent's surface. Ionic strength is one of the key factors affecting the electrical double-layer (EDL) structure of a hydrated particulate. An increase in ionic strength leads to a decrease in EDL thickness and an increase in the amount of indifferent ions approaching the

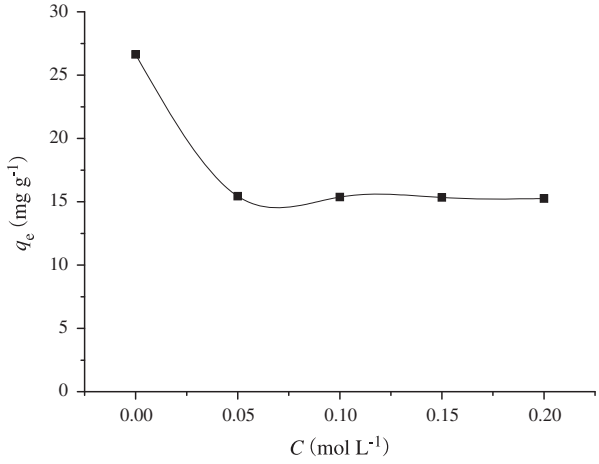

Fig. 5. The effect of salt concentration on adsorption quantity ($C_0 = 30$ mg L^{-1}, CCS dosage 1.0 g L^{-1}, pH 4.00, contact time 720 min, and $T = 303$ K).

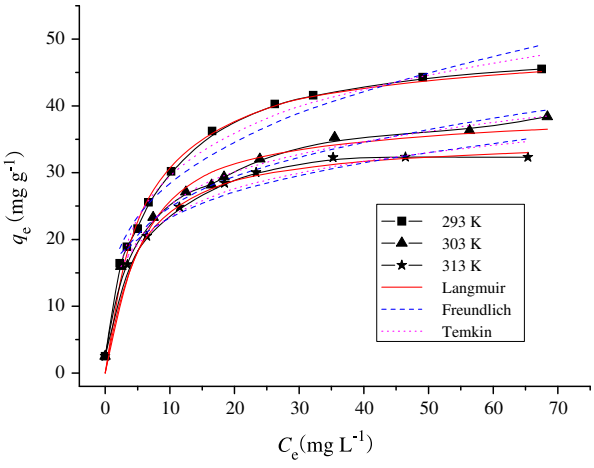

Fig. 6. Adsorption isotherms and the nonlinear fitted curves of three isotherm models at different temperatures.

adsorbent surface. Thus, the results shown above can be attributed in part to increased competition between MO and Cl^- ions for surface sites with increasing the ionic strength [48]. Usually, salt may screen the electrostatic interaction of opposite charges in adsorbents and the dye molecules, and an increase in salt concentration could decrease the amount of dye adsorbed, confirming that electrostatic interaction was responsible for the adsorption of MO by chitosan [25]. Another reason is that when ionic strength increase the activity (effective concentration) of MO the active sites decrease, so the adsorptive capacity of MO onto adsorbents decreases [11,49]. This phenomenon implied that the interaction mechanism between MO and CCS includes ion exchange or electrostatic attraction.

3.5. The effect of equilibrium concentration on adsorption

The effect of the initial concentration of MO at different temperatures on adsorption was shown in Fig. 6.

It was seen from the Fig. 6 that equilibrium uptake of MO increased gradually with the increase of MO concentration at the same temperature until it reaches equilibrium, this is the result of the molecular collision opportunities between adsorbate and adsorbent enhanced along with MO concentration increased. Higher MO concentration can provide driving force to overcome the resistance of the adsorption. Adsorption quantity did not change with the concentration increase to a certain level because the active sites of the adsorbent surface were fully occupied and the adsorption equilibrium was reached. It was observed from Fig. 6 that higher temperature was not favor of MO adsorption and this implied that the adsorption process be exothermic.

The nonlinear fitted curves with three adsorption models were also shown in Fig. 6, respectively. The Langmuir, Freundlich, and Temkin adsorption constants evaluated from the isotherms at different temperatures and the values of R^2 and SAE were presented in Table 1.

Langmuir constant q_m represents the monolayer saturation at equilibrium, reduced with increase in temperature. However, the values of K_L represented the opposite trend, which accounts for the exothermic nature of the adsorption process.

The Freundlich model was employed to fit the equilibrium data for further analysis. The decrease of Freundlich constant K_F with increase of temperature confirmed that adsorption was favorable at low temperatures and the process was exothermic in nature. Values of $1/n$ ranged between 0.1 and 0.5, which indicated that the adsorption readily and easily occurred in the experimental conditions [50].

For Temkin model, the parameters of A increased and B decreased along with the rise of temperature. Parameter B can reflect the heat of adsorption. The results also showed the exothermic process.

Based on the values of R^2, SAE in Table 1 and the fitted curves in Fig. 6, higher determined coefficients ($R^2 > 0.97$) and smaller errors (SAE < 10.4) for the Langmuir model and the Temkin model at all tested temperature values suggested that these two models be available for describing the adsorption of MO onto CCS. However, the Freundlich isotherm was not satisfactory for fitting the adsorption data compared with Langmuir and the Temkin model. These showed that

Table 1
Parameters of adsorption isotherm models at different temperatures

T/K	293 K	303 K	313 K
Langmuir			
q_m (mg g^{-1})	49.0	39.1	35.2
K_L (L mg^{-1})	0.175	0.203	0.230
R^2	0.990	0.974	0.989
SAE	10.4	13.7	6.65
Freundlich			
K_F (mg g^{-1})	14.8	14.51	14.2
$1/n$	0.284	0.236	0.215
R^2	0.954	0.971	0.908
SAE	19.6	8.39	12.1
Temkin			
A	8.27	9.89	10.0
B	9.33	6.76	5.89
R^2	0.993	0.996	0.976
SAE	10.3	4.13	8.60

Note: SAE $= \sum_{i=1}^{n} |q_c - q_e|$, q_c is the calculated date according to the adsorption model, n is number of experimental points.

the adsorption may be monolayer adsorption. Langmuir isotherm model fitted the results quite well and suggested that the surface of the adsorbent be homogenous, while Temkin isotherm model fitted well and suggested that the surface be heterogeneous. The results showed that the process of adsorption was complex and chemical action and physical action were both existed.

3.6. Kinetic studies

The effects of contact time on adsorption quantity at various MO concentrations were illustrated in Fig. 7.

As seen in Fig. 7, the dye adsorption process on the CCS was rapid in the first 50 min, then continued with a slower rate during the 60–360 min and nearly reached a plateau after approximately 600 min of the experiment. A two-stage kinetic process is evident: an initial rapid stage, where adsorption rate is fast and contributes significantly to equilibrium uptake, and a slower second stage which is relatively small to the contribution of the total MO adsorption. The first stage is the instantaneous adsorption stage or external surface adsorption. The second stage is the gradual adsorption stage (where the intra-particle diffusion is rate controlled) and finally MO uptake reaches equilibrium. This suggests that adsorption include two diffusion processes, external and internal diffusion.

The calculated kinetic parameters, correlation coefficient, and errors were listed in Table 2.

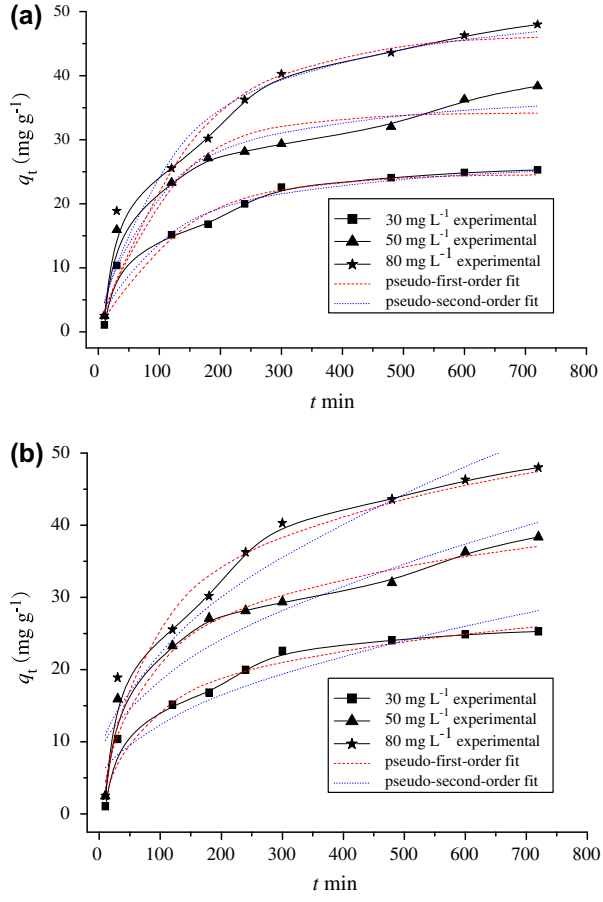

Fig. 7. Adsorption kinetic and the nonlinear fitted curves ((a) pseudo-first-order kinetic model and pseudo-second-order model (b) Elovich model and intra-particle diffusion model) of four models at different concentrations.

It was observed from Table 2 that the kinetic data were fitted in order as the Elovich, pseudo-second-order, pseudo-first-order and intra-particle diffusion. The Elovich model was best to describe the adsorption of MO because of the largest R^2 value ($R^2 > 0.987$) and lowest errors (SAE < 10.0). The constant α increased and diffusion rate constant β diminished along with the increase of MO concentration. Furthermore, the fitted curves from the Elovich were most near to the experimental curve (shown in Fig. 7). As the Elovich equation is successfully used to describe the adsorption kinetics of ion exchange systems, it can be concluded that the adsorption system be a chemical process, especially an ion exchange process [40].

Pseudo-second-order equation can also be used to describe MO/CCS adsorption of for the higher determined coefficient and values of q_e from model was close to experimental data. This indicated that the adsorption reaction belonged to the chemical

Table 2
Kinetic parameters for adsorption of MO onto CCS at different concentrations

C_0 (mg L^{-1})	30	50	80
Pseudo-first-order			
k_1 (min^{-1})	0.00802	0.00971	0.00692
$q_{e\text{-}cal}$ (mg g^{-1})	24.6	34.2	46.3
$q_{e\text{-}exp}$ (mg g^{-1})	25.3	38.3	48.0
R^2	0.936	0.901	0.932
SAE	4.46	15.1	8.05
Pseudo-second-order			
$k_2 \times 10^{-4}$ (g mg^{-1} min^{-1})	3.90	3.50	1.70
$q_{e\text{-}cal}$ (mg g^{-1})	28.2	38.8	53.9
R^2	0.960	0.950	0.955
SAE	10.3	18.0	19.1
Elovich			
α	0.825	1.36	1.45
β	0.179	0.131	0.0974
R^2	0.989	0.989	0.988
SAE	4.98	6.13	10.0
Intra-particle diffusion			
K_t	0.926	1.27	1.74
C	3.50	6.18	5.42
R^2	0.883	0.889	0.917
SAE	19.6	26.0	29.3

adsorption reaction process [39]. The equilibrium q_e increased and the rate constant k_2 decreased with the concentration increase, are probably because the increase of the initial concentration of the solution made the number of dye molecules to increase, caused the space block. From Table 2, pseudo-first-order equation can also better describe the adsorption process.

The adsorbates are most probably transported from the bulk phase into the adsorbent through the intra-particle diffusion, which is the rate-determining step in rapidly stirred batch reactors [46]. If the plot of q_t vs. t passes through the origin then the intra-particle diffusion is the only rate-limiting step. Intra-particle diffusion equation was available according to values of R^2 listed in Table 2 and fitted curves from Fig. 7. These implied that intra-particle diffusion play a significant role in the uptake of MO ions by CCS. The parameters of C in Table 2 were not zero and this showed that intra-particle diffusion was involved in the adsorption process, but it was not the sole rate-controlling step. Both external diffusion and intra-particle diffusion play an important role during the adsorption process.

3.7. Desorption and regeneration

Regeneration of exhausted adsorbent and reuse are of importance due to environmental- and economic motivations [51–53]. Desorption and regeneration studies are important in the field of adsorption studies. The results of regeneration efficiency were listed in Table 3.

From Table 3, regeneration efficiency was found to be highest (99.9%) in case of $NaClO_3$ and other methods was over 94%. However, considering the high cost and separation of oxidation by-product generated in the progress, hot water (333 K) can be used as a regenerating agent as the regeneration efficiency can reach 96.9%, which was attributed to the previous study that the increase of temperature was unfavorable for the adsorption of MO (but contributed to desorption). In addition, the desorption method of hot water was economically feasible, environmental friendly and made it possible for large-scale promotion of CCS.

3.8. Thermodynamic studies

In practical environmental engineering, both enthalpy and entropy must be taken into consideration in order to determine what processes occur spontaneously. Thermodynamics parameters, Gibbs free energy (ΔG°), enthalpy (ΔH°), and entropy (ΔS°) were calculated by van't Hoff and Gibb's-Helmholtz equations [50]:

$$K_C = \frac{C_{ad,e}}{C_e} \tag{10}$$

$$\Delta G^\circ = -RT \ln K_c \tag{11}$$

$$\Delta G^\circ = \Delta H^\circ - T\Delta S^\circ \tag{12}$$

where $C_{ad,e}$ and C_e are the equilibrium concentrations of dye (mg g^{-1}) on the adsorbent and solution, respectively. K_c is the equilibrium constant, the value of K_c in the lowest experimental dye concentration can be obtained. T is the solution temperature (K) and R is the gas constant.

Thermodynamic parameters were calculated and shown in Table 4.

The negative ΔG° values at different temperatures revealed the spontaneity and feasibility of the adsorption process. The decrease in the value of the free

Table 3
Regeneration efficiency with various methods

Method	Hot water	NaOH	Hot NaCl	$NaClO_3$
Efficiency/%	96.9	94.4	97.3	99.9

Table 4
Thermodynamic parameters of MO adsorption onto CCS

T/K	293	303	313
ΔG° (kJ mol^{-1})	−4.87	−4.74	−3.85
ΔH° (kJ mol^{-1})		−19.9	
ΔS° (J mol^{-1} K^{-1})		−50.9	

energy with increase in the temperature indicated that it was in favor of adsorption at lower temperature. The negative ΔH° value confirmed the exothermic adsorption process. The negative value of ΔS° which was very small suggested the hardly change randomness at the solid–solution interface during the adsorption of MO onto CCS. The encounter ions which were displaced by the adsorbate species gained smaller translational entropy than ions lost by adsorbate, thus allowing for nonprevalence of randomness in the system.

3.9. Mechanism of adsorption

The functional groups such as $-NH_2$, –OH, originally presented in chitosan, were intact after coating on quartz sand and were available for interaction with dye molecules. Chitosan was potential as an adsorbent for the removal of anionic dyes from textile wastewater because it efficiently adsorbed dyes at acidic condition (amine groups $-NH_2$ protonated as $-NH_3^+$) [25,54]. In aqueous solutions, the synthetic reactive dye, including MO, is dissolved and the sulfonate group of the reactive dye is dissociated and converted to anionic ions:

$$DSO_3Na \xrightarrow{H_2O} DSO_3^- + Na^+ \quad (13)$$

The adsorption process then proceeds due to the electrostatic interaction between these two counter ions and forms an ion pair [54]. As a result, these ion pairs can act as anion adsorption sites

$$R' - NH_3^+ + DSO_3^- \Leftrightarrow R' - NH_3^+ - O_3SD \quad (14)$$

This result demonstrated an ion exchange mechanism.

At a higher pH value, the surface charge of chitosan is neutral or negative which hinders adsorption by the decrease of static attraction or increase of electrostatic force of repulsion between the negatively charged dye molecule and adsorbent. But there is still some adsorption capacity at pH over 7. Therefore, in addition to ionic bonding, there may be a strong possibility that dye molecules with N, S, and O acts through hydrogen bonding with $-CH_2OH$ groups in the polysaccharide chain of the chitosan unit [55]. This suggests the involvement of other interactions as hydrogen bonds, van der Waals force, etc. in the adsorption process [56,57]. The effect of initial pH, elution studies, and the thermodynamic parameters demonstrated that MO was probably adsorbed onto chitosan by both physical and chemical adsorptions. In addition, the adsorption mechanism under acidic conditions was chemical adsorption, while under caustic conditions was both physical and chemical adsorptions [58]. Fig. 8 represents the possible interactions between chitosan and MO.

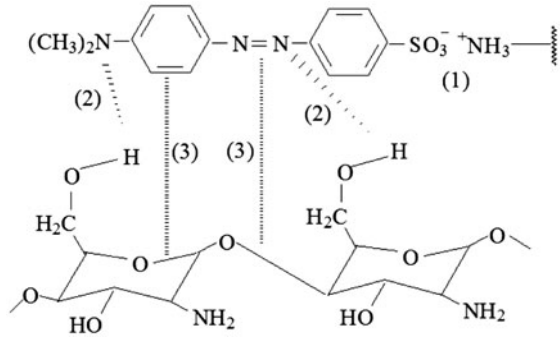

Fig. 8. MO–chitosan interaction: (1) ionic interaction (involves pH of experimental solution 4), (2) hydrogen bonding between the hydroxyl group of chitosan and electronegative element in the dye molecule, and (3) van der Waals force.

4. Conclusion

Adsorption property of MO onto CCS was studied in batch mode. It was in favor of adsorption at solution pH 4.0. The high temperature and salt co-existed in solution were not beneficial for MO adsorption. The Langmuir model fitted the equilibrium data well and the adsorption quantity from Langmuir model was to 49.0 mg g^{-1} at 293 K. The kinetic process of MO adsorption can be best predicted by Elovich equation. The results implied that ion exchange be the main mechanism. The thermodynamics parameters indicated that the adsorption process was spontaneous and exothermal. Finally, the desorption study indicated that the regeneration efficiency was over 90% by several methods. Therefore, it may be concluded that the CCS can be an efficient, environmental, and economically feasible alternative for the removal of anionic dye from wastewater.

Acknowledgments

This work was supported by the National Natural Science Foundation of China for undergraduate cultivation in basic science (J1210060).

References

[1] C.I. Pearce, J.R. Lloyd, J.T. Guthrie, The removal of colour from textile wastewater using whole bacterial cells: A review, Dyes Pigm. 58 (2003) 179–196.
[2] G. McMullan, C. Meehan, A. Conneely, N. Kirby, T. Robinson, P. Nigam, I.M. Banat, R. Marchant, W.F. Smyth, Microbial decolourisation and degradation of textile dyes, Appl. Microbiol. Biotechnol. 56 (2001) 81–87.
[3] G. Crini, Non-conventional low-cost adsorbents for dye removal: A review, Bioresour. Technol. 97 (2006) 1061–1085.
[4] Z. Badani, H. Ait-Amar, A. Si-Salah, M. Brik, W. Fuchs, Treatment of textile waste water by membrane bioreactor and reuse, Desalination 185 (2005) 411–417.
[5] S.H. Lin, C.M. Lin, Treatment of textile waste effluents by ozonation and chemical coagulation, Water Res. 27 (1993) 1743–1748.
[6] H.N. Bhatti, N. Akhtar, N. Saleem, Adsorptive removal of methylene blue by low-cost *Citrus sinensis* Bagasse: equilibrium, kinetic and thermodynamic characterization, Arab. J. Sci. Eng. 37 (2012) 9–18.
[7] Z. Aksu, Application of biosorption for the removal of organic pollutants: A review, Process Biochem. 40 (2005) 997–1026.
[8] M. Asgher, H.N. Bhatti, Mechanistic and kinetic evaluation of biosorption of reactive azo dyes by free, immobilized and chemically treated *Citrus sinensis* waste biomass, Ecol. Eng. 36 (2010) 1660–1665.
[9] A. Mittal, V. Thakur, J. Mittal, H. Vardhan, Process development for the removal of hazardous anionic azo dye Congo red from wastewater by using hen feather as potential adsorbent, Desalin. Water Treat. 52 (2014) 227–237.
[10] H.N. Bhatti, Y. Safai, Removal of anionic dyes by rice milling waste from synthetic effluents: Equilibrium and thermodynamic studies, Desalin. Water Treat. 48 (2012) 267–277.
[11] R.P. Han, W.H. Zou, W.H. Yu, S.J. Cheng, Y.F. Wang, J. Shi, Biosorption of methylene blue from aqueous solution by fallen phoenix tree's leaves, J. Hazard. Mater. 141 (2007) 156–162.
[12] S. Noreen, H.N. Bhatti, S. Nausheen, S. Sadaf, M. Ashfaq, Batch and fixed bed adsorption study for the removal of Drimarine Black CL-B dye from aqueous solution using a lignocellulosic waste: A cost affective adsorbent, Ind. Crops Prod. 50 (2013) 568–579.
[13] J.Y. Song, W.H. Zou, Y.Y. Bian, F.Y. Su, R.P. Han, Adsorption characteristics of methylene blue by peanut husk in batch and column mode, Desalination 265 (2011) 119–125.
[14] M. Asgher, H.N. Bhatti, Removal of reactive blue 19 and reactive blue 49 textile dyes by citrus waste biomass from aqueous solution: equilibrium and kinetic study, Can. J. Chem. Eng. 90 (2012) 413–419.
[15] Y.Y. Su, B.L. Zhao, W. Xiao, R.P. Han, Adsorption behavior of light green anionic dye using cationic surfactant modified wheat straw in batch and column mode, Environ. Sci. Pollut. Res. 20 (2013) 5558–5568.
[16] R.P. Han, D.D. Ding, Y.F. Xu, W.H. Zou, Y.F. Wang, Y.F. Li, L.N. Zou, Use of rice husk for the adsorption of Congo red from aqueous solution in column mode, Bioresour. Technol. 99 (2008) 2938–2946.
[17] C.H. Xu, J.J. Shi, W.Z. Zhou, B.Y. Gao, Q.Y. Yue, X.H. Wang, Bromate removal from aqueous solutions by nano crystalline akaganeite (β-FeOOH)-coated quartz sand (CACQS), Chem. Eng. J. 187 (2012) 63–68.
[18] H.M. Guo, D. Stüben, Z. Berner, Arsenic removal from water using natural iron mineral–quartz sand columns, Sci. Tot. Environ. 377 (2007) 142–151.
[19] M. Arias, J.D. Silva-Carballal, L. García-Rio, J. Mejut, A. Nunez, Retention of phosphorus by iron and aluminum-oxides-coated quartz particles, J. Colloid Interface Sci. 295 (2006) 65–70.
[20] R.P. Han, W.H. Zou, Z.P. Zhang, J. Shi, J.J. Yang, Removal of copper(II) and lead(II) from aqueous solution by manganese oxide coated sand – I. Characterization and kinetic study, J. Hazard. Mater. 137 (2006) 384–395.
[21] M.N.V.R. Kumar, A review of chitin and chitosan applications, React. Funct. Polym. 46 (2000) 1–27.
[22] E. Guibal, Interactions of metal ions with chitosan-based sorbents: A review, Sep. Purif. Technol. 38 (2004) 43–74.
[23] P. Miretzky, A.F. Cirelli, Hg(II) removal from water by chitosan and chitosan derivatives: A review, J. Hazard. Mater. 167 (2009) 10–23.
[24] J.R. Rangel-Mendez, R. Monroy-Zepeda, E. Leyva-Ramos, P.E. Diaz-Flores, K. Shirai, Chitosan selectivity for removing cadmium (II), copper (II), and lead (II) from aqueous phase: pH and organic matter effect, J. Hazard. Mater. 162 (2009) 503–511.
[25] G. Crini, P.M. Badot, Application of chitosan, a natural aminopolysaccharide, for dye removal from aqueous solutions by adsorption processes using batch studies: A review of recent literature, Prog. Polym. Sci. 33 (2008) 399–447.
[26] N.K. Lazaridis, G.Z. Kyzas, A.A. Vassiliou, D.N. Bikiaris, Chitosan derivatives as biosorbents for basic dyes, Langmuir 23 (2007) 7634–7643.
[27] W.S.W. Ngah, N.F.M. Ariff, M.A.K.M. Hanafiah, Preparation, characterization and environmental application of cross-linked chitosan-coated bentonite for tartrazine adsorption from aqueous solution, Water Air Soil Pollut. 206 (2010) 225–236.
[28] C.M. Futalan, C.C. Kan, M.L. Dalida, C. Pascua, M.W. Wan, Fixed-bed column studies on the removal of copper using chitosan immobilized on bentonite, Carbohydr. Polym. 83 (2011) 697–704.
[29] S. Hasan, A. Krishnaiah, T.K. Ghosh, D.S. Viswanath, V.M. Boddu, E.D. Smith, Adsorption of divalent cadmium (Cd(II)) from aqueous solutions onto chitosan-coated perlite beads, Ind. Eng. Chem. Res. 45 (2006) 5066–5077.
[30] L. Wang, A.Q. Wang, Adsorption characteristics of Congo red onto the chitosan/montmorillonite nanocomposite, J. Hazard. Mater. 147 (2007) 979–985.
[31] M.Y. Chang, R.S. Juang, Adsorption of tannic acid, humic acid, and dyes from water using the composite of chitosan and activated clay, J. Colloid Interface Sci. 278 (2004) 18–25.

[32] Y. Vijaya, S.R. Popuri, V.M. Boddu, A. Krishnaiah, Modified chitosan and calcium alginate biopolymer sorbents for removal of nickel (II) through adsorption, Carbohydr. Polym. 72 (2008) 261–271.
[33] W.S. Wan Ngah, L.C. Teong, R.H. Toh, M.A.K.M. Hanafiah, Utilization of chitosan–zeolite composite in the removal of Cu(II) from aqueous solution: adsorption, desorption and fixed bed column studies, Chem. Eng. J. 209 (2012) 46–53.
[34] H.M. Zhu, M.M. Zhang, Y.Q. Liu, L.J. Zhang, R.P. Han, Study of Congo red adsorption onto chitosan coated magnetic iron oxide in batch mode, Desalin. Water Treat. 37 (2012) 46–54.
[35] M.W. Wan, I.G. Petrisor, H.T. Lai, D. Kim, T.F. Yen, Copper adsorption through chitosan immobilized on sand to demonstrate the feasibility for *in situ* soil decontamination, Carbohydr. Polym. 55 (2004) 249–254.
[36] M.W. Wan, C.C. Kan, B.D. Rogel, M.L.P. Dalida, Adsorption of copper (II) and lead (II) ions from aqueous solution on chitosan-coated sand, Carbohydr. Polym. 80 (2010) 891–899.
[37] K.Y. Foo, B.H. Hameed, Insights into the modeling of adsorption isotherm systems, Chem. Eng. J. 156 (2010) 2–10.
[38] Y.S. Ho, G. McKay, The kinetics of sorption of divalent metal ions onto *Sphagnum moss* peat, Water Res. 34 (2000) 735–742.
[39] Y.S. Ho, G. McKay, Pseudo-second order model for sorption processes, Process Biochem. 34 (1999) 451–465.
[40] C.W. Cheung, J.F. Porter, G. McKay, Sorption kinetics for the removal of copper and zinc from effluents using bone char, Sep. Purif. Technol. 19 (2000) 55–64.
[41] W.J. Weber Jr., J.C. Morris, Kinetics of adsorption on carbon from solution, J. Sanit. Eng. Div. ASCE 89 (1963) 31–59.
[42] R.P. Han, Y. Wang, Q. Sun, L.L. Wang, J.Y. Song, X.T. He, C.C. Dou, Malachite green adsorption onto natural zeolite and reuse by microwave irradiation, J. Hazard. Mater. 175 (2010) 1056–1061.
[43] Z.W. Wang, P. Han, Y.B. Jiao, X.T. He, C.C. Dou, R.P. Han, Adsorption of Congo red using ethylenediamine modified wheat straw, Desalin. Water Treat. 30 (2011) 195–206.
[44] A. Mittal, J. Mittal, A. Malviya, D. Kaur, V.K. Gupta, Decoloration treatment of a hazardous triarylmethane dye, light green SF (yellowish) by waste material adsorbents, J. Colloid Interface Sci. 342 (2010) 518–527.
[45] S.B. Wang, Z.H. Zhu, A. Coomes, F. Haghseresht, G.Q. Lu, The physical and surface chemical characteristics of activated carbons and the adsorption of methylene blue from wastewater, J. Colloid Interface Sci. 284 (2005) 440–446.
[46] V.K. Gupta, D. Pathania, S. Sharma, P. Singh, Preparation of bio-based porous carbon by microwave assisted phosphoric acid activation and its use for adsorption of Cr(VI), J. Colloid Interface Sci. 401 (2013) 125–132.
[47] T.K. Saha, N.C. Bhoumik, S. Karmaker, M.G. Ahmed, H. Ichikawa, Y. Fukumori, Adsorption of methyl orange onto chitosan from aqueous solution, J. Water Resour. Prot. 02 (2010) 898–906.
[48] C.H. Weng, Y.T. Lin, T.W. Tzeng, Removal of methylene blue from aqueous solution by adsorption onto pineapple leaf powder, J. Hazard. Mater. 170 (2009) 417–424.
[49] A. Tabak, N. Baltas, B. Afsin, M. Emirik, B. Caglar, E. Eren, Adsorption of reactive red 120 from aqueous solutions by cetylpyridinium-bentonite, J. Chem. Technol. Biotechnol. 85 (2010) 1199–1207.
[50] Z. Aksu, Determination of the equilibrium, kinetic and thermodynamic parameters of the batch biosorption of nickel(II) ions onto *Chlorella vulgaris*, Process Biochem. 38 (2002) 89–99.
[51] V.K. Gupta, A. Mittal, D. Jhare, J. Mittal, Batch and bulk removal of hazardous colouring agent rose Bengal by adsorption techniques using bottom ash as adsorbent, RSC Adv. 2 (2012) 8381–8389.
[52] Y.K. Li, B.L. Zhao, L.J. Zhang, R.P. Han, Biosorption of copper ion by natural and modified wheat straw in fixed-bed column, Desalin. Water Treat. 51 (2013) 5735–5745.
[53] M. Asgher, H.N. Bhatti, Evaluation of thermodynamics and effect of chemical treatments on sorption potential of Citrus waste biomass for removal of anionic dyes from aqueous solutions, Ecol. Eng. 38 (2012) 79–85.
[54] Y.C. Wong, Y.S. Szeto, W.H. Cheung, G. McKay, A dsorption of acid dyes on chitosan equilibrium isotherm analyses, Process Biochem. 39 (2004) 693–702.
[55] J.H. An, S. Dultz, Adsorption of tannic acid on chitosan-montmorillonite as a function of pH and surface charge properties, Appl. Clay Sci. 36 (2007) 256–264.
[56] S. Chatterjee, S. Chatterjee, B.P. Chatterjee, A.K. Guha, Adsorptive removal of Congo red, a carcinogenic textile dye by chitosan hydrobeads: Binding mechanism, equilibrium and kinetics, Colloids Surf., A: Physicochem. Eng. Aspects 299 (2007) 146–152.
[57] Y.C. Wong, Y.S. Szeto, W.H. Cheung, G. McKay, Equilibrium studies for acid dye adsorption onto chitosan, Langmuir 19 (2003) 7888–7894.
[58] N. Sakkayawong, P. Thiravetyan, W. Nakbanpote, Adsorption mechanism of synthetic reactive dye wastewater by chitosan, J. Colloid Interface Sci. 286 (2005) 36–42.